

Thermodynamics to infer the astrophysics of binary black hole mergers

Patrick Hu,¹ Karan Jani,¹ Kelly Holley-Bockelmann,¹ and Gregorio Carullo^{2,3}

¹*Department Physics and Astronomy, Vanderbilt University,
2301 Vanderbilt Place, Nashville, TN, 37235, USA*

²*Dipartimento di Fisica “Enrico Fermi”, Università di Pisa, Pisa I-56127, Italy*

³*INFN sezione di Pisa, Pisa I-56127, Italy*

We introduce the Merger Entropy Index (\mathcal{I}_{BBH}), a new parameter to measure the efficiency of entropy transfer for any generic binary black hole merger in General Relativity. We find that \mathcal{I}_{BBH} is bounded between an asymptotic maximum and minimum. For the observed population of mergers detected by LIGO [1] and Virgo [2], we find that \mathcal{I}_{BBH} is $\lesssim 30\%$ of its theoretical maximum. By imposing the thermodynamical consistency between the pre- and post-merger states through \mathcal{I}_{BBH} , we showcase **BRAHMA** – a novel framework to infer the properties and astrophysical implications of gravitational-wave detections. For GW190521 – the heaviest confirmed binary black hole merger observed so far – our framework rules out high mass-ratio, negative effective inspiral spin, and electromagnetic counterpart claims. Furthermore, our analysis provides an independent confirmation that GW190521 belongs to a separate population.

Entropy transfer.— A binary black hole (BBH) merger [3], regardless of its astrophysical origins, is an irreversible process. From the Second Law of Thermodynamics, the merger inevitably leads to an increase of entropy, ΔS_{BBH} , in the Universe:

$$\Delta S_{\text{BBH}} \equiv S_f - (S_1 + S_2) \geq 0, \quad (1)$$

where S_f is the entropy of the remnant black hole formed after merger, and S_1, S_2 are the entropies of the two pre-merger black holes. According to the laws of black hole mechanics [4], this change in entropy is a function of the mass and spin magnitudes of black holes before ($m_{1,2}, |\chi_{1,2}|$) and after merger ($m_f, |\chi_f|$). For the family of Kerr black holes [5], the entropy can be measured as:

$$S_i = \frac{2\pi G}{c\hbar} m_i^2 \left(1 + \sqrt{1 - |\chi_i|^2}\right). \quad (2)$$

We construct a mass-invariant ratio, ϵ_S , to quantify the entropy transfer during the coalescence of BBH from its pre- to post-merger stage, and note that it must be bracketed as follows:

$$\epsilon_{S,\text{min}} \leq \epsilon_S \equiv \frac{S_f}{S_1 + S_2} \leq \epsilon_{S,\text{max}}, \quad (3)$$

where $\epsilon_{S,\text{max}}$ and $\epsilon_{S,\text{min}} = 1$ are the global maximum and minimum of entropy transfer across the BBH parameter space $\Lambda(q, \chi_1, \chi_2)$ with $q = m_2/m_1 \leq 1$.

Global Maximum for BBH Entropy.— By inserting Eq. (2) in Eq. (3), we find that entropy transfer has a leading order term equal to $(1+q)^2/(1+q^2)$. Therefore, the entropy transfer will be larger for equal-mass BBH mergers ($q=1$). Instead, it is in the extreme mass-ratio limit ($q \rightarrow 0$) of BBH mergers that $\epsilon_S \rightarrow 1$.

To acquire an understanding of the dependence of ϵ_S on $\Lambda(q, \chi_1, \chi_2)$, and obtain an estimate of $\epsilon_{S,\text{max}}$, it is useful to first specialise to mergers of comparable masses

($q \simeq 1$) and spins ($|\chi_{1,2}| \simeq \chi$). In this case, the entropy transfer can be approximated as:

$$\epsilon_S \approx 2(1 - E_{\text{rad}})^2 \left(\frac{1 + \sqrt{1 - |\mathbf{J} - \mathbf{J}_{\text{rad}}|^2}}{1 + \sqrt{1 - \chi^2}} \right), \quad (4)$$

where $\mathbf{J} = \chi_1 + \chi_2 + \mathbf{L}$ is the total angular momentum in the pre-merger system, \mathbf{L} is the corresponding orbital angular momentum, and E_{rad} and \mathbf{J}_{rad} are the energy and angular momentum radiated to infinity via gravitational waves. The radiated quantities and angular momentum are expressed here in dimensionless units, and normalized with binary mass ($M = m_1 + m_2$).

Based on Eq. (4), if a BBH coalescence radiates more energy, it would lead to a smaller change in entropy. If there is no residual angular momentum after the merger, it would lead to a higher change in entropy. First noted by Hawking [6], the theoretical maximum energy that can be radiated in the comparable mass and spin case is $E_{\text{rad}} = 1/2$. A minimum entropy transfer would require a binary with two maximally spinning black holes ($\chi \rightarrow 1$) to radiate all the angular momentum ($\mathbf{J}_{\text{rad}} \sim \mathbf{J}$). In this case, Eq. (4) approaches $\epsilon_{S,\text{min}}$. However, there exist no configurations in the Λ hyperspace satisfying such a conditions. In fact, numerical relativity simulations find that BBH systems are unable to radiate more than $\sim 10\%$ rest mass [7–9]. Thus, for near equal-mass BBH systems, the entropy transfer is *always* greater than the lower-bound imposed by the Second Law.

For generic quasi-circular BBH systems, E_{rad} and \mathbf{J}_{rad} are strongly dependent on the mass-ratio q , spin vectors $\chi_{1,2}$ and their orientation with respect to \mathbf{L} . The radiated quantities dictates the mass and spin of the black hole formed after the merger [10], and consequently, the final entropy S_f . To find the global maximum for quasi-circular BBHs, we numerically solve Eq. (3) across the Λ hyperspace. We utilize the phenomenological fits of E_{rad} and \mathbf{J}_{rad} [11–13]. These fits are calibrated on numerical relativity simulations of BBH mergers [7, 9],

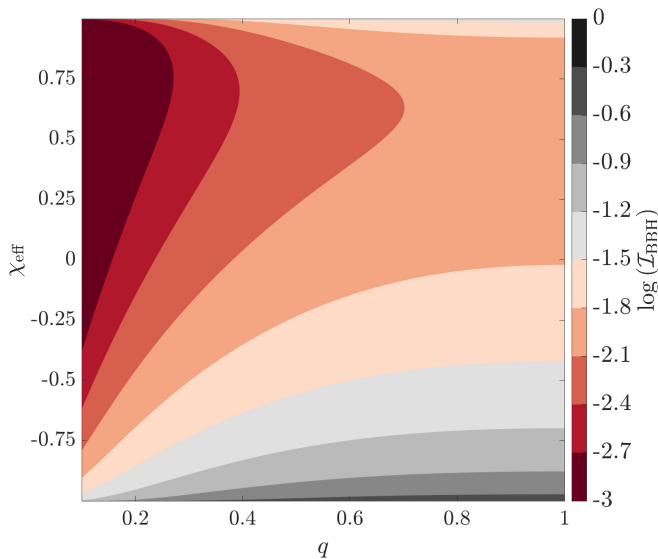


FIG. 1. Global behavior of Merger Entropy Index (\mathcal{I}_{BBH}) within the intrinsic BBH parameter space, Λ . For demonstration, this figure only shows non-precessing binaries with equal spin vectors.

which incorporate the apparent horizon framework [14]. We find good agreement on $\epsilon_{S,\text{max}}$ between the two different fits employed, $\epsilon_{S,\text{max}} = 3.6235$ from [11], and $\epsilon_{S,\text{max}} = 3.6342$ from [13]. As expected, $\epsilon_{S,\text{max}}$ occurs for a system of equal-mass, maximally spinning black holes, aligned in the direction opposite that of the orbital angular momentum.

For the special case of head-on collisions ($L \sim 0$) of equal-mass BBHs, the entropy transfer can, in principle, be even higher. Suppose a collision occurs between two maximally spinning black holes that are anti-aligned with each other ($J \sim 0$). Provided the collision *radiates no energy* ($E_{\text{rad}} \sim 0$), only then, Eq. (4) would approach a theoretical upper-bound of $\epsilon_{S,\text{max}} = 4$. However, based on numerical relativity simulations, we can infer that such collisions would emit $\gtrsim 1.35\%$ of rest mass. Thus, a subset of highly eccentric, maximally spinning, equal-mass mergers can approach an entropy transfer in the range $3.62 \lesssim \epsilon_{S,\text{max}} \lesssim 3.91$.

Merger Entropy Index.— By using the bounds of ϵ_S , we construct the Merger Entropy Index as,

$$\mathcal{I}_{\text{BBH}} \equiv \frac{\pi \Delta S_{\text{BBH}}}{9 S_1 + S_2}. \quad (5)$$

This index measures the efficiency of entropy transfer during a BBH coalescence. All BBH systems in General Relativity will satisfy $\mathcal{I}_{\text{BBH}} \in (0, 1]$. By construction, the index is mass-invariant and is thus applicable to a wide range of astrophysical scenarios. For all astrophysical binaries, we anticipate $\mathcal{I}_{\text{BBH}} \lesssim 0.9$.

Fig. 1 shows the global behavior of Merger Entropy Index within a slice in the hyperspace Λ , the intrinsic

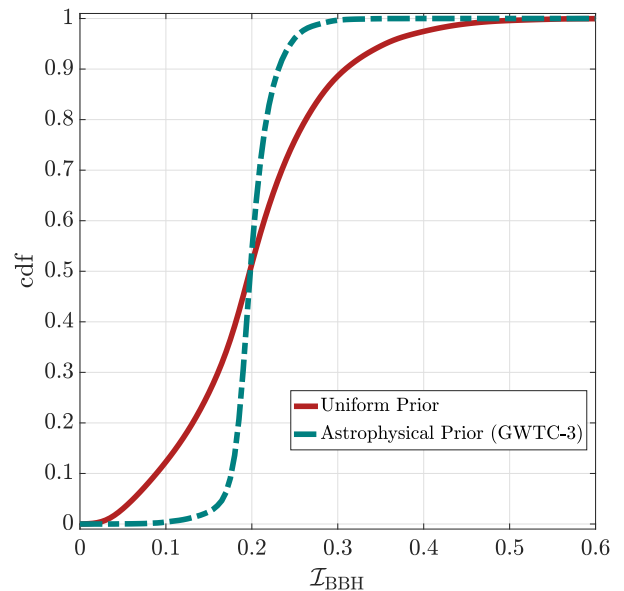


FIG. 2. Cumulative distribution of Merger Entropy Index for a uniform prior within the intrinsic BBH parameter space Λ (red curve). The dotted green curve is for region of Λ derived from the observed population of BBH by LIGO-Virgo [16]

BBH parameters. We employ RIT fits [11] to compute \mathcal{I}_{BBH} , which are valid for quasi-circular to moderately eccentric BBHs. If these BBHs are non-spinning, we find that $\mathcal{I}_{\text{BBH}} \propto q/(1+q)^2 \equiv \eta$, the symmetric mass-ratio.

For near equal-mass BBHs, the index has a rather strong dependence on the orientation of spin vectors. When the effective inspiral spin parameter (χ_{eff}) [15] is negative, \mathcal{I}_{BBH} exponentially approaches to 0.9. On the contrary, when χ_{eff} is positive, \mathcal{I}_{BBH} has very limited variance of $\sim 20\%$. This is consistent regardless of the mass-ratio of the system. For high mass-ratio BBHs with high primary BH spin, the index exponentially scales to the lower-bound of 0. We note that BBHs with high in-plane spins is that they tend to have high \mathcal{I}_{BBH} .

In Fig. 2, we show the cumulative distribution of \mathcal{I}_{BBH} across the intrinsic BBH parameter space Λ . The red curve is induced by a uniform distribution within mass-ratios $1/q \in [1, 20]$, spin magnitudes $\chi_{1,2} \in [0, 0.99]$ and cosine of the spin orientations $\cos\theta_{1,2} \in [-1, 1]$. This induced distribution is a good representation of the default prior for the Merger Entropy Index for quasi-circular BBH mergers in General Relativity. When assuming the uniform prior, $\mathcal{I}_{\text{BBH}} \lesssim 0.5$ at 99% credibility, greatly restricting its allowed range. This is consistent with Fig. 1, which shows that higher values of \mathcal{I}_{BBH} are confined in a small domain of Λ .

The dotted green curve in Figure 3 shows a distribution of \mathcal{I}_{BBH} drawn out of an *astrophysical prior*. This prior is derived directly from the constraints on the masses and spins for the observed population of BBH mergers in GWTC-3 [16] from the LIGO-Virgo detectors. In

particular, we use the distribution $p(q) \propto q^\beta$ from `PowerLaw+Peak Model` to fetch the mass-ratio, and the `Gaussian Spin Model` for the distribution of black hole spin magnitudes and orientations. For the astrophysical prior, we find \mathcal{I}_{BBH} is steeply centered around 0.2. There are no values $\gtrsim 0.3$ with 99% confidence interval.

From the distributions discussed above, we can infer the Merger Entropy Index has an upper-bound as:

$$0 \leq \mathcal{I}_{\text{BBH}} \lesssim \begin{cases} 1.0 & \text{Theoretical Limits;} \\ 0.5 & \text{Uniform Prior;} \\ 0.3 & \text{Astrophysical Prior} \end{cases} \quad (6)$$

While the theoretical and uniform prior bounds of \mathcal{I}_{BBH} in Eq. (6) are independent of the BBH origins, the astrophysical bounds could well vary between the supermassive and stellar mass BBH population, and would be interesting to explore in future work. We found that KS-convergence can confidently differentiate (with a probability of one part in billion) between the LIGO-Virgo derived distribution of \mathcal{I}_{BBH} [16] from the uniform prior distribution. This suggests \mathcal{I}_{BBH} can be an effective tool to test astrophysical formation channels.

Novel GW Framework.— By adopting the Merger Entropy Index, we introduce a generalized framework called **BRAHMA** (**B**ina**R**y **bl**ack **H**oles **M**erger entropy **A**nalysis). The schematic flow of BRAHMA is shown in Fig. 3. Every BBH detection whose pre- (S_1, S_2) and post-merger (S_f) entropies have been independently measured (e.g. because models with different physical content have been used to infer them) have to satisfy the upper and lower bounds of the theoretical limits of \mathcal{I}_{BBH} from Eq. (6). This is under the assumption that the observed BBH population is consistent with the predictions of General Relativity, which by now has a strong experimental support [17–19]. With the current generation of gravitational-wave data analysis tools, the pre-merger entropy will typically be measured by conducting a Bayesian analysis over the intrinsic Λ (masses, spins) and extrinsic Θ (distance, orientation, sky-location) BBH parameter space with inspiral-merger-ringdown (IMR) waveform models (green wavelet in Fig. 3). For the post-merger entropy, our framework strictly requires an independent measurement of the black hole ringdown (pink wavelet in Fig. 3), which is achieved by an independent measurement of the post-merger properties [17–19]. See Ref. [20] for thermodynamical constraints on the information emission process of LIGO-Virgo BHs using post-merger measurements.

From the posterior distributions of pre-merger entropies (with size $1 \times m$) and post-merger entropies ($1 \times n$), we compute a Merger Entropy Index matrix ($m \times n$). Assuming the detected BBH is consistent with General Relativity, every element in the matrix has to satisfy (pass) theoretical bounds stated in Equation (6).

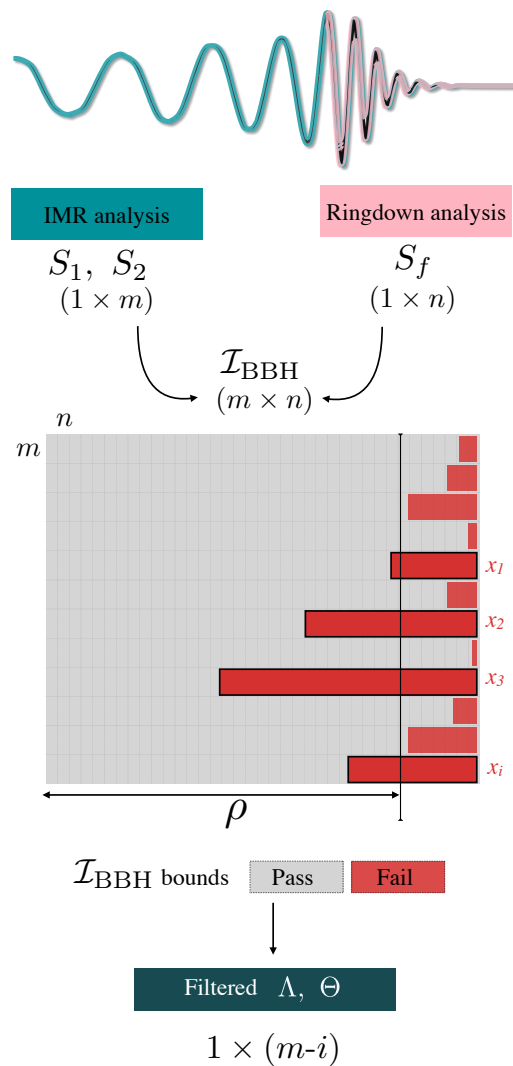


FIG. 3. Schematic diagram of BRAHMA Framework. We use a BBH detection (wavelet at the top) whose pre- and post-merger states have been independently measured. From this information we compute the Merger Entropy Index matrix. By imposing the bounds of \mathcal{I}_{BBH} stated in Equation (6), we filter parts of the inspiral posterior distribution (rows in the figure) which *pass* this criterion with $\geq \rho\%$.

For illustration, we show them as grey boxes of \mathcal{I}_{BBH} in the matrix in Figure 3. The matrix may contain some *failed* elements, i.e they do not obey the \mathcal{I}_{BBH} bounds (shown in the Fig. 3 as red boxes). For every row in the \mathcal{I}_{BBH} matrix, we compute the the fraction of *passed* columns to that of the total elements in the column (n). If this fraction is less than the threshold ρ , we discard this row vector and filter the pre-merger distribution to a new length $1 \times (m - i)$. As a default setting in our framework, we fix $\rho = 90\%$. BRAHMA directly filters the parameter space constrained by the IMR model. All the BBH inspiral parameters, including extrinsic (Θ) ones, are now further constrained than the original output

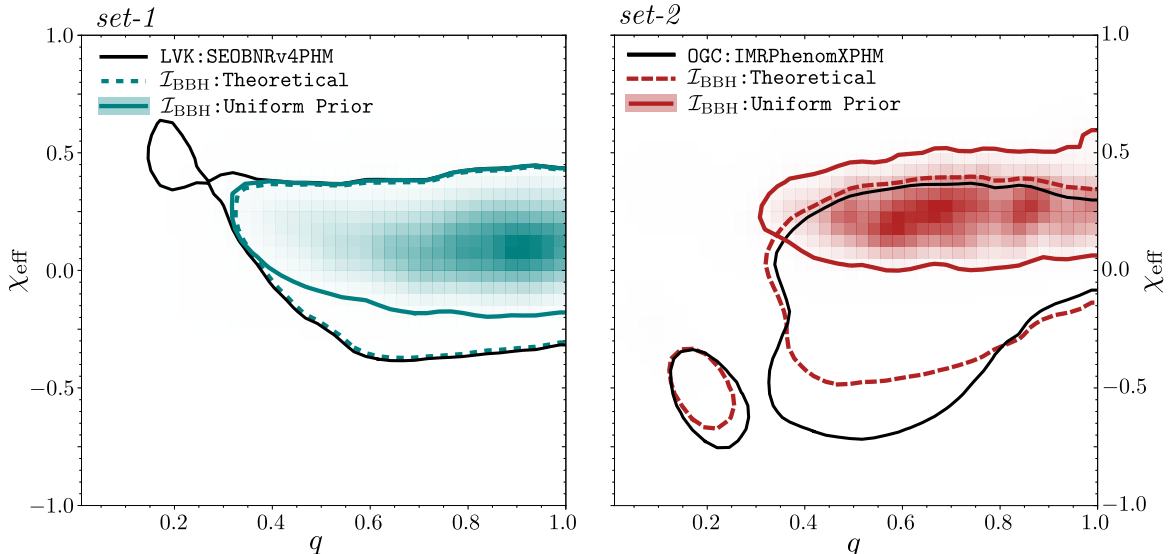


FIG. 4. New constraints on GW190521’s mass-ratio and effective spins using BRAHMA *Left*: Constraints using the pre- and post-merger measurement from *set-1*, i.e. the LIGO-Virgo-KAGRA Collaboration (LVK). The black curve refers to the published distribution from the SEOBNRv4PHM model. The dashed green line shows the constraints we obtain in BRAHMA by imposing theoretical bounds of \mathcal{I}_{BBH} . The filled green contour is the constraint from BRAHMA for a uniform prior bound of \mathcal{I}_{BBH} . *Right*: Constraints using pre- and post-merger measurement from *set-2*, i.e. the Open Gravitational-Wave Catalog (OGC). The black curve refers to the published distribution from the IMRPhenomXPHM model. The red dashed and red contour refers to the constraints obtained from BRAHMA by imposing theoretical and uniform prior bounds of \mathcal{I}_{BBH} on this set. The two-dimensional curves show the 90% credible regions.

from the Bayesian analysis, even though BRAHMA does not explicitly require any direct information on most of these parameters (e.g. luminosity distance, coalescence phase). Naturally, the constraints on BBH parameters are tighter if the bounds on the Merger Entropy Index are set from a uniform or astrophysical prior, compared to the most general theoretical limit.

The framework is built on the idea that for certain systems, post-merger analyses provide a more robust measurement of the end state properties than full-signal analyses. This situation can happen when full-signal models do not correctly represent complete solutions of the Einstein equations (i.e. they are “unfaithful” to accurate numerical simulation of BBHs), or when they lack the inclusion of certain physical effects. The post-merger stage is generally simpler to model regardless of the pre-merger history of the BBH system, and that the agnostic post-merger models employed in our analysis do not rely on numerical calibration to quasi-circular mergers. For example, eccentricity effects are much less relevant in the post-merger due to fast binary circularisation in the late stages of the pre-merger dynamics, see Fig. 4 of [21]. On the contrary, pre-merger models employed by the LVK collaboration currently cannot incorporate astrophysically interesting scenarios such as eccentric orbits, dynamical captures and high-mass ratio precessing binaries. Some progress in some of these directions has been recently obtained

using Effective One Body models for non-precessing eccentric systems and eccentric dynamical captures [22, 23]. However, such templates currently lack the inclusion of BHs spins and higher harmonics.

Applications to GW190521.— To demonstrate the application of our BRAHMA framework, we apply it to the parameters measurements of GW190521. This event has been shown to suffer from systematic uncertainties of its pre-merger properties [23–26], thus falling in the category of systems to which our framework is especially relevant. Detected during the third observing run of the LIGO and Virgo detectors, this event marks the first direct measurement of an intermediate-mass black hole [27], though its astrophysical formation remains so far mysterious [28]. Such massive BBHs have an advantage of an independent measurement of the remnant mass and spin (m_f, χ_f) from the ringdown stage [29]. Several studies have performed a full Bayesian inference on the pre- and post-merger properties of GW190521 using a variety of gravitational waveform models and numerical relativity simulations [28, 30–33]. From these data products, we chose two fully independent set of measurements to test BRAHMA:

set-1: We choose the waveform model SEOBNRv4PHM [34] to measure the pre-merger entropies (S_1, S_2). We do so using its posteriors on detector-frame masses (m_1, m_2) and spin magnitudes

Parameter	<i>set-1:</i>		<i>set-2:</i>	
	LVK:SEOB-PHM	With BRAHMA	OGC:IMR-XPHM	With BRAHMA
Lower-bound on q	0.32	0.39	0.22	0.37
Lower-bound on χ_{eff}	-0.28	-0.12	-0.60	+0.06
Probability($z \leq \text{AGN}$)	10%	7%	41%	5%

TABLE I. Source properties for GW190521 with \mathcal{I}_{BBH} framework and imposing uniform prior. For mass-ratio q and effective inspiral spin χ_{eff} , we provide the lower-bound at the 90% confidence interval. The third row is the cumulative probability for the inferred redshift z to be equal or less than the one from the claimed AGN flare, J1249+349 [44].

(χ_1, χ_2), available from the Gravitational-Wave Open Science Center (GWOSC) maintained by the LIGO-Virgo-KAGRA Collaboration [35]. These pre-merger constraints were obtained with the Bayesian parameter scheme RIFT [36]. For the post-merger entropy (S_f), we use the posteriors on the remnant mass and spin (m_f, χ_f) obtained through the pyRing analysis framework [37] with the Kerr₂₂₂ model [28, 38]. This template incorporates the $\ell = m = 2$ quasi-normal modes up to the second overtone ($n = 0, 1, 2$), and is applied starting at the peak of the waveform (a proxy for the *merger*). Among the post-merger models employed in [28], it provides the most precise measurements of ringdown, and thus that of remnant mass and spin.

set-2: From the Open Gravitational Catalog (OGC) [39], which is an independent analysis on the open data, we get the pre-merger estimates for the IMRPhenomXPHM waveform model [40]. Their analysis is performed using the Bayesian code pyCBC Inference [41]. The post-merger estimates are obtained from a Kerr template [42] incorporating the $(\ell, m, n) = \{(2, 2, 0), (3, 3, 0)\}$ modes, as there is claimed evidence for both these ringdown modes in GW190521 [43].

As shown in the two panels of Fig. 4-5, the inference of pre-merger properties by these two sets is significantly different (compare the black curves in left-right panels). However, both the sets provide support for (i) an asymmetric mass distribution ($q \lesssim 0.3$), (ii) negative effective inspiral spins ($\chi_{\text{eff}} \lesssim -0.2$) and (iii) a source redshift that overlaps with an AGN flare, J1249+349 [44]. These features carry strong implications for the astrophysical origins of GW190521. By applying our BRAHMA framework, we find that both *set-1* and *set-2* no longer provides evidence for the features (i)-(iii). Table I summarizes the overall improvement in pre-merger properties of GW190521 using BRAHMA.

After applying the **theoretical** prior of \mathcal{I}_{BBH} in BRAHMA, *set-1* (LVK:SEOB-PHM) no longer shows the bimodality in $q - \chi_{\text{eff}}$ parameter space. For *set-2*

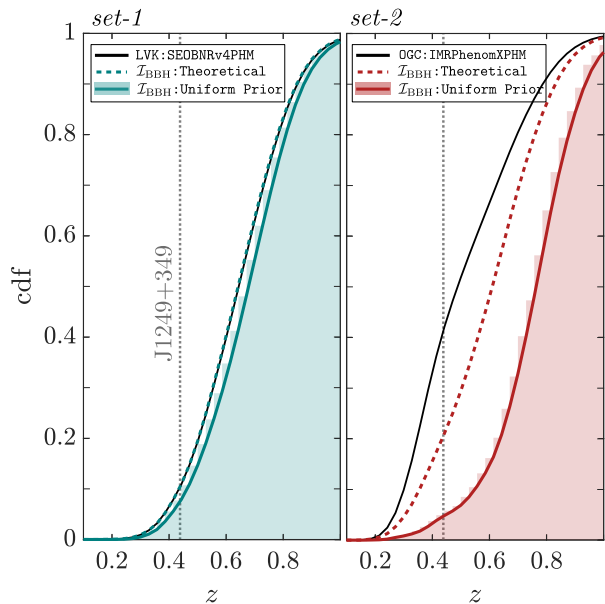


FIG. 5. New constraints on the redshift of GW190521 using the BRAHMA framework. The color coding on both the panels is same as Figure 4. The dotted grey line refers to the redshift of the electromagnetic candidate observed by the ZTF collaboration [44].

(OGC:IMR-XPHM), the bimodality still remains, however, the support for $\chi_{\text{eff}} \lesssim 0$ is significantly lower (see dashed lines in Fig. 4). These bounds also have significant impact on the source redshift for *set-2*, dropping its cumulative probability at $z \leq 0.438$ (electromagnetic candidate claim) by a factor of ~ 2 , confirming GW190521 is farther than the claimed electromagnetic candidate.

When the **uniform prior** bounds are adopted in BRAHMA, we see a significant reduction in the 90% confidence intervals in both the sets. The most notable changes appear in our constraint from *set-2* on the effective inspiral spin of GW190521, which suggests the parameter is positive with 90% confidence. Also, for the same set the cumulative probability for source redshift at $z \leq 0.438$ drops to $\sim 5\%$ (a factor of 8). Filtered posteriors from both sets no longer show any bimodality, and in fact, converge to similar a post-merger distribution after applying our \mathcal{I}_{BBH} framework. Moreover, the distribution from these two sets now seems consistent with other waveform models that have analyzed GW190521 [28], suggesting a possible improvement in waveform systematic with \mathcal{I}_{BBH} .

By imposing the **astrophysical prior** in BRAHMA, we find that 99.9% (95%) of pre-merger distribution is filtered out from *set-2* (*set-1*). This provides an additional confirmation that GW190521 is at the tail end of the astrophysical population derived from all other LIGO-Virgo black holes [16].

Conclusion.— We introduce a new thermodynamical formalism into gravitational-wave astrophysics. For the current generation detectors, we find our formalism is particularly powerful for probing GW190521-like lower-range intermediate-mass black holes ($\sim 10^{2-3} M_{\odot}$) [45, 46]. Our framework is applicable to BBH lying in regions of the parameter space where full numerical simulations are not extensively available and for which the pre- and post-merger states can be independently measured, for all mass ranges. Our formalism will be even more germane for next-generation detectors Cosmic Explorer [47], Einstein Telescope [48], upcoming space-mission LISA [49] and potential deci-Hertz experiments [50, 51], as we expect the post-merger measurements to be more often and louder. Future work will explore the implications of the Merger Entropy Index (\mathcal{I}_{BBH}) and the BRAHMA framework on BBH demographics, formation channels and gravitational waveform systematics.

ACKNOWLEDGMENTS

We thank Maximiliano Isi and Nathan Johnson-McDaniel for useful comments. P.H.’s research was supported by the Immersion Initiative at Vanderbilt University. K.J and K.H.B.’s research was supported by the Stevenson Chair endowment funds at Vanderbilt University.

This material is based upon work supported by NSF’s LIGO Laboratory which is a major facility fully funded by the National Science Foundation. This research has made use of data, software and/or web tools obtained from the Gravitational Wave Open Science Center (<https://www.gw-openscience.org/>), a service of LIGO Laboratory, the LIGO Scientific Collaboration and the Virgo Collaboration. LIGO Laboratory and Advanced LIGO are funded by the United States National Science Foundation (NSF) as well as the Science and Technology Facilities Council (STFC) of the United Kingdom, the Max-Planck-Society (MPS), and the State of Niedersachsen/Germany for support of the construction of Advanced LIGO and construction and operation of the GEO600 detector. Additional support for Advanced LIGO was provided by the Australian Research Council. Virgo is funded, through the European Gravitational Observatory (EGO), by the French Centre National de Recherche Scientifique (CNRS), the Italian Istituto Nazionale di Fisica Nucleare (INFN) and the Dutch Nikhef, with contributions by institutions from Belgium, Germany, Greece, Hungary, Ireland, Japan, Monaco, Poland, Portugal, Spain.

[1] LIGO Scientific Collaboration, *Classical and Quantum*

- Gravity* **32**, 074001 (2015), arXiv:1411.4547 [gr-qc].
- [2] Virgo Collaboration, *Classical and Quantum Gravity* **32**, 024001 (2015), arXiv:1408.3978 [gr-qc].
- [3] LIGO Scientific Collaboration and Virgo Collaboration, *Physical Review Letters* **116**, 061102 (2016), arXiv:1602.03837 [gr-qc].
- [4] J. M. Bardeen, B. Carter, and S. W. Hawking, *Communications in Mathematical Physics* **31**, 161 (1973).
- [5] J. D. Bekenstein, *Phys. Rev. D* **7**, 2333 (1973).
- [6] S. W. Hawking, *Phys. Rev. Lett.* **26**, 1344 (1971).
- [7] A. H. Mroué, M. A. Scheel, B. Szilágyi, H. P. Pfeiffer, M. Boyle, D. A. Hemberger, L. E. Kidder, G. Lovelace, S. Ossokine, N. W. Taylor, A. Zenginoğlu, L. T. Buchman, T. Chu, E. Foley, M. Giesler, R. Owen, and S. A. Teukolsky, *Physical Review Letters* **111**, 241104 (2013).
- [8] K. Jani *et al.*, *Classical and Quantum Gravity* **33**, 204001 (2016).
- [9] J. Healy, C. O. Lousto, Y. Zlochower, and M. Campanelli, *Classical and Quantum Gravity* **34**, 224001 (2017).
- [10] E. Barausse and L. Rezzolla, *Astrophys.J.* **704**, L40 (2009), arXiv:0904.2577 [gr-qc].
- [11] J. Healy, C. O. Lousto, and Y. Zlochower, *Phys.Rev.* **D90**, 104004 (2014), arXiv:1406.7295 [gr-qc].
- [12] N. K. Johnson-McDaniel, A. Gupta, D. Keitel, P. Ajith, O. Birnholtz, F. Ohme, and S. Husa, *LIGO DCC*, *LIGO-T1600168-v6* (2016).
- [13] V. Varma, S. E. Field, M. A. Scheel, J. Blackman, D. Gerosa, L. C. Stein, L. E. Kidder, and H. P. Pfeiffer, *Phys. Rev. Research* **1**, 033015 (2019).
- [14] O. Dreyer, B. Krishnan, D. Shoemaker, and E. Schnetter, *Phys. Rev. D* **67**, 024018 (2003).
- [15] Y. Pan, A. Buonanno, M. Boyle, L. T. Buchman, L. E. Kidder, H. P. Pfeiffer, and M. A. Scheel, *Phys. Rev. D* **84**, 124052 (2011).
- [16] The LIGO Scientific Collaboration, The Virgo Collaboration, and The KAGRA Scientific Collaboration, arXiv e-prints, arXiv:2111.03634 (2021), arXiv:2111.03634 [astro-ph.HE].
- [17] G. Carullo, *Phys. Rev. D* **103**, 124043 (2021), arXiv:2102.05939 [gr-qc].
- [18] M. Isi, W. M. Farr, M. Giesler, M. A. Scheel, and S. A. Teukolsky, *Physical Review Letters* **127** (2021), 10.1103/physrevlett.127.011103.
- [19] R. Abbott, T. Abbott, S. Abraham, F. Acernese, K. Ackley, A. Adams, C. Adams, R. Adhikari, V. Adya, C. Affeldt, and et al., *Physical Review D* **103** (2021), 10.1103/physrevd.103.122002.
- [20] G. Carullo, D. Laghi, J. Veitch, and W. Del Pozzo, *Phys. Rev. Lett.* **126**, 161102 (2021), arXiv:2103.06167 [gr-qc].
- [21] E. A. Huerta *et al.*, *Phys. Rev. D* **100**, 064003 (2019), arXiv:1901.07038 [gr-qc].
- [22] A. Nagar, P. Rettegno, R. Gamba, and S. Bernuzzi, *Phys. Rev. D* **103**, 064013 (2021), arXiv:2009.12857 [gr-qc].
- [23] R. Gamba, M. Breschi, G. Carullo, P. Rettegno, S. Albanesi, S. Bernuzzi, and A. Nagar, (2021), arXiv:2106.05575 [gr-qc].
- [24] I. M. Romero-Shaw, P. D. Lasky, E. Thrane, and J. C. Bustillo, *Astrophys. J. Lett.* **903**, L5 (2020), arXiv:2009.04771 [astro-ph.HE].
- [25] J. C. Bustillo, N. Sanchis-Gual, A. Torres-Forné, and

- J. A. Font, *Phys. Rev. Lett.* **126**, 201101 (2021), [arXiv:2009.01066 \[gr-qc\]](#).
- [26] J. C. Bustillo, N. Sanchis-Gual, A. Torres-Forné, J. A. Font, A. Vajpeyi, R. Smith, C. Herdeiro, E. Radu, and S. H. W. Leong, *Phys. Rev. Lett.* **126**, 081101 (2021), [arXiv:2009.05376 \[gr-qc\]](#).
- [27] LIGO Scientific Collaboration and Virgo Collaboration, *Phys. Rev. Lett.* **125**, 101102 (2020), [arXiv:2009.01075 \[gr-qc\]](#).
- [28] R. Abbott, T. D. Abbott, S. Abraham, F. Acernese, K. Ackley, C. Adams, R. X. Adhikari, V. B. Adya, C. Affeldt, M. Agathos, and et al., *The Astrophysical Journal* **900**, L13 (2020).
- [29] G. Carullo, W. Del Pozzo, and J. Veitch, *Physical Review D* **99** (2019), [10.1103/physrevd.99.123029](#).
- [30] I. Romero-Shaw, P. D. Lasky, E. Thrane, and J. Calderón Bustillo, *Astrophys. J. Lett* **903**, L5 (2020), [arXiv:2009.04771 \[astro-ph.HE\]](#).
- [31] A. H. Nitz and C. D. Capano, *The Astrophysical Journal* **907**, L9 (2021).
- [32] H. Estellés, S. Husa, M. Colleoni, M. Mateu-Lucena, M. de Lluc Planas, C. García-Quirós, D. Keitel, A. Ramos-Buades, A. K. Mehta, A. Buonanno, and S. Ossokine, arXiv e-prints , [arXiv:2105.06360 \(2021\)](#), [arXiv:2105.06360 \[gr-qc\]](#).
- [33] V. Gayathri, J. Healy, J. Lange, B. O'Brien, M. Szczepanczyk, I. Bartos, M. Campanelli, S. Klimentko, C. Lousto, and R. O'Shaughnessy, arXiv e-prints , [arXiv:2009.05461 \(2020\)](#), [arXiv:2009.05461 \[astro-ph.HE\]](#).
- [34] S. Ossokine, A. Buonanno, S. Marsat, R. Cotesta, S. Babak, T. Dietrich, R. Haas, I. Hinder, H. P. Pfeiffer, M. Pürrer, and et al., *Physical Review D* **102** (2020), [10.1103/physrevd.102.044055](#).
- [35] R. Abbott *et al.*, *SoftwareX* **13**, 100658 (2021).
- [36] J. Lange, R. O'Shaughnessy, and M. Rizzo, "Rapid and accurate parameter inference for coalescing, precessing compact binaries," (2018), [arXiv:1805.10457 \[gr-qc\]](#).
- [37] G. C. et al., "pyRing: a time-domain ringdown analysis python package," <https://git.ligo.org/lscsoft/pyring>.
- [38] M. Giesler, M. Isi, M. A. Scheel, and S. Teukolsky, *Phys. Rev. X* **9**, 041060 (2019), [arXiv:1903.08284 \[gr-qc\]](#).
- [39] A. H. Nitz, C. D. Capano, S. Kumar, Y.-F. Wang, S. Kastha, M. Schäfer, R. Dhurkunde, and M. Cabero, arXiv e-prints , [arXiv:2105.09151 \(2021\)](#), [arXiv:2105.09151 \[astro-ph.HE\]](#).
- [40] G. Pratten, C. García-Quirós, M. Colleoni, A. Ramos-Buades, H. Estellés, M. Mateu-Lucena, R. Jaume, M. Haney, D. Keitel, J. E. Thompson, and et al., *Physical Review D* **103** (2021), [10.1103/physrevd.103.104056](#).
- [41] C. M. Biwer, C. D. Capano, S. De, M. Cabero, D. A. Brown, A. H. Nitz, and V. Raymond, *Publications of the Astronomical Society of the Pacific* **131**, 024503 (2019).
- [42] R. Abbott *et al.* (LIGO Scientific, Virgo), *Phys. Rev. D* **103**, 122002 (2021), [arXiv:2010.14529 \[gr-qc\]](#).
- [43] C. D. Capano, M. Cabero, J. Westerweck, J. Abedi, S. Kastha, A. H. Nitz, A. B. Nielsen, and B. Krishnan, arXiv e-prints , [arXiv:2105.05238 \(2021\)](#), [arXiv:2105.05238 \[gr-qc\]](#).
- [44] M. Graham, K. Ford, B. McKernan, N. Ross, D. Stern, K. Burdge, M. Coughlin, S. Djorgovski, A. Drake, D. Duev, and et al., *Physical Review Letters* **124** (2020), [10.1103/physrevlett.124.251102](#).
- [45] K. Jani, D. Shoemaker, and C. Cutler, *Nature Astronomy* **4**, 260 (2020), [arXiv:1908.04985 \[gr-qc\]](#).
- [46] The LIGO Scientific Collaboration, the Virgo Collaboration, and the KAGRA Collaboration, arXiv e-prints , [arXiv:2105.15120 \(2021\)](#), [arXiv:2105.15120 \[astro-ph.HE\]](#).
- [47] D. Reitze *et al.*, arXiv e-prints , [arXiv:1907.04833 \(2019\)](#), [arXiv:1907.04833 \[astro-ph.IM\]](#).
- [48] M. Punturo *et al.*, *Proceedings, 14th Workshop on Gravitational wave data analysis (GWDAW-14): Rome, Italy, January 26-29, 2010*, *Class. Quant. Grav.* **27**, 194002 (2010).
- [49] P. Amaro-Seoane *et al.*, arXiv e-prints , [arXiv:1702.00786 \(2017\)](#), [arXiv:1702.00786 \[astro-ph.IM\]](#).
- [50] S. Sato *et al.*, *Journal of Physics: Conference Series* **840**, 012010 (2017).
- [51] K. Jani and A. Loeb, *Journal of Cosmology and Astroparticle Physics* **2021**, 044 (2021).